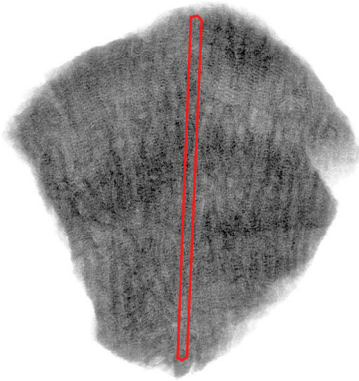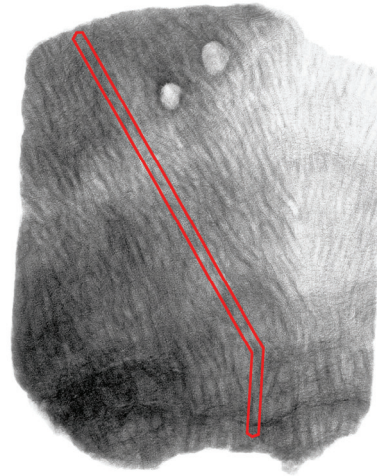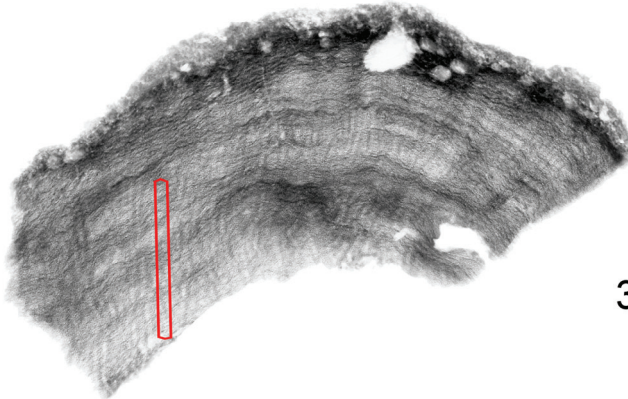325-31A-2R-CC (5-10)
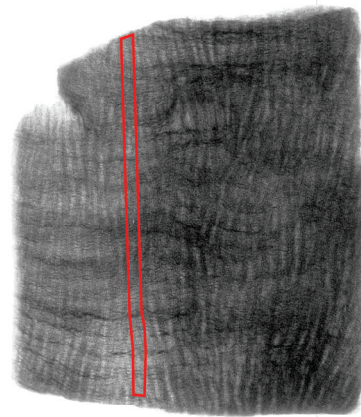
325-33A-7R-CC (2-10)

325-36A-16R-1 (12-22)

325-53A-9R-CC (0-7)

325-39A-15R-1 (22-25)

5 cm
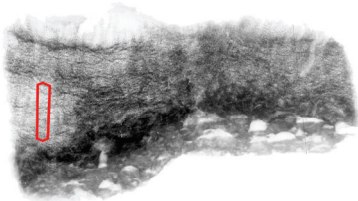
Supplementary Figure 1. X-radiograph images of fossil Great Barrier Reef corals.
X-radiograph positive prints of slabbed *Isopora palifera*/*cuneata* corals reveal generally
well preserved skeletons. Skeletal areas of obvious diagenetic alteration were not
microsampled. The microsampling transect for each coral is indicated in red. **a,** Corals
microsampled at subseasonal resolution. **b,** Corals microsampled for bulk composition.
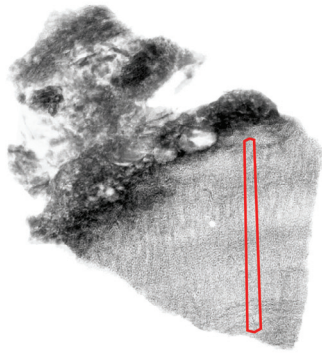
325-53A-15R-1 (33-37)   325-57A-5R-1 (126-133)

5 cm
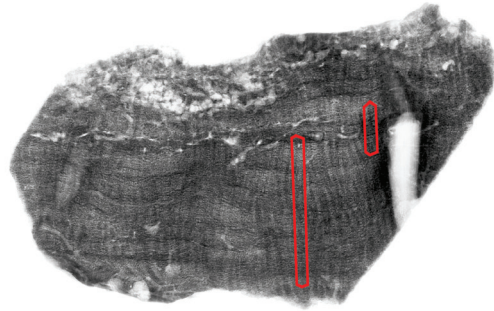
Supplementary Figure 1, a (continued).

325-31A-2R-1 (27-32)

325-31A-7R-1 (16-24)

325-33A-5R-1 (68-74)
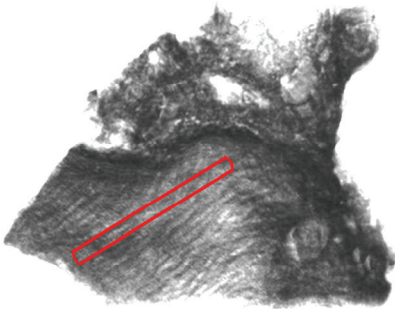
325-33A-9R-1 (7-16)

325-33A-8R-1 (11-17)

5 cm

Supplementary Figure 1, b.

325-33A-10R-1 (42-48)
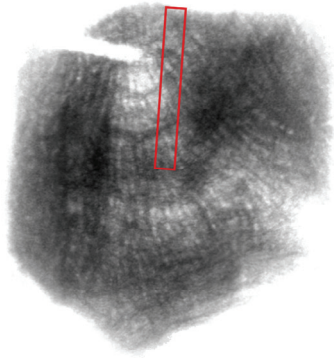
325-33A-16R-1 (54-60)

325-35A-3R-1 (35-38)
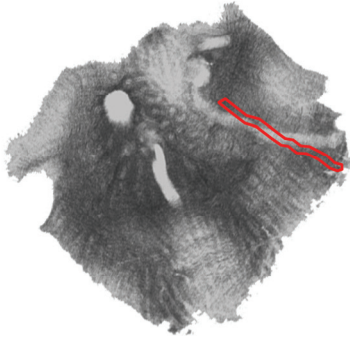
325-36A-16R-1 (6-10)

325-53A-6R-1 (7-9)

325-53A-15R-1 (30-33)

5 cm
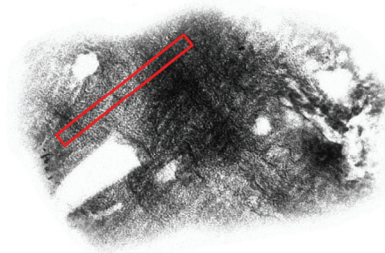
Supplementary Figure 1, b (continued).

325-53A-15R-1 (42-48)
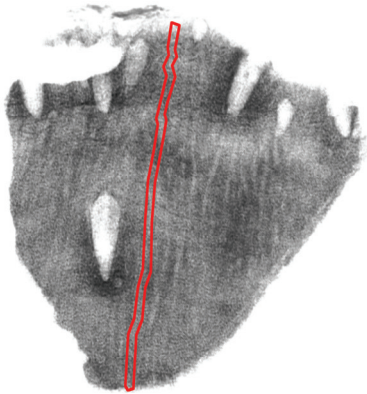
325-57A-4R-1 (75-88)
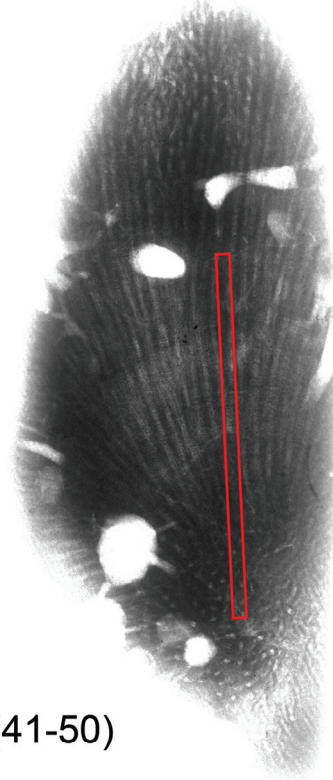
325-57A-5R-1 (1-3)
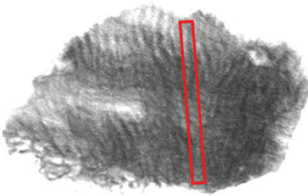
325-57A-5R-1 (41-50)

5 cm
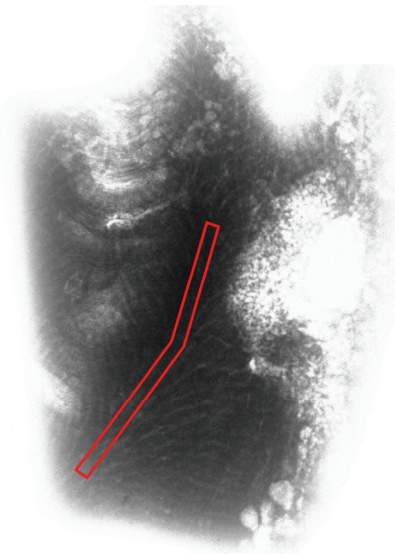
Supplementary Figure 1, b (continued).

325-57A-5R-1 (115-122)
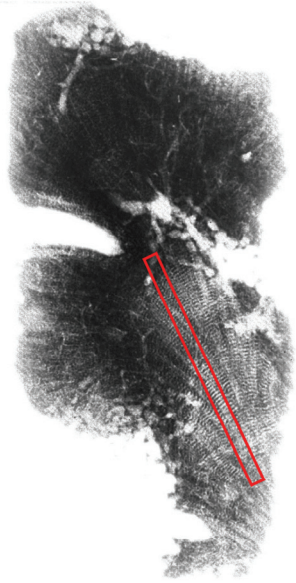
325-57A-6R-1 (103-114)

325-57A-6R-2 (66-80)

5 cm
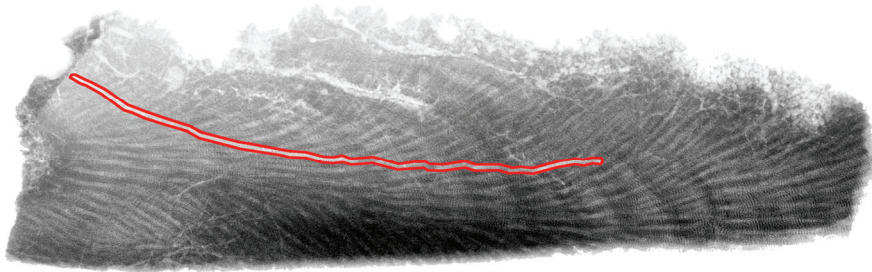
Supplementary Figure 1, b (continued).

325-31A-2R-CC (5-10)
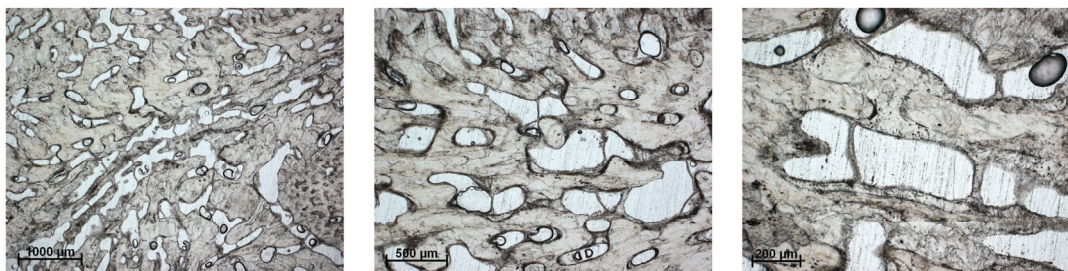
325-33A-7R-CC (2-10)
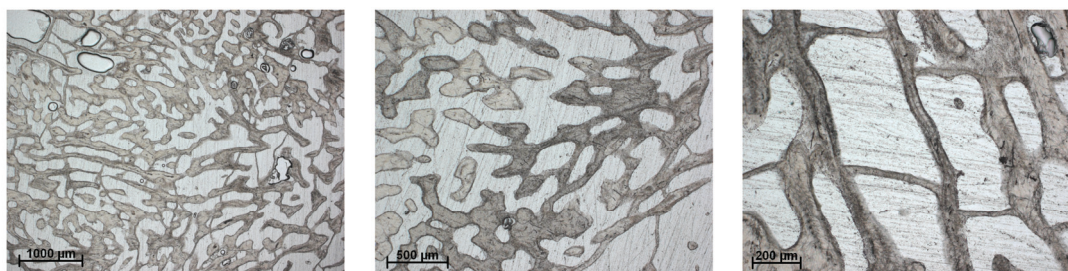
325-36A-16R-1 (12-22)
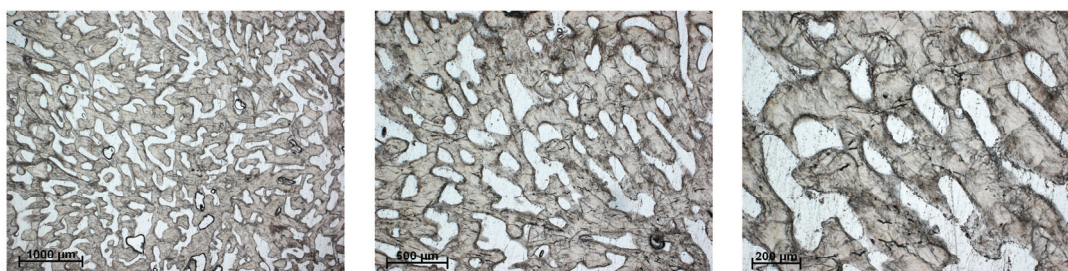
325-39A-15R-1 (22-25)
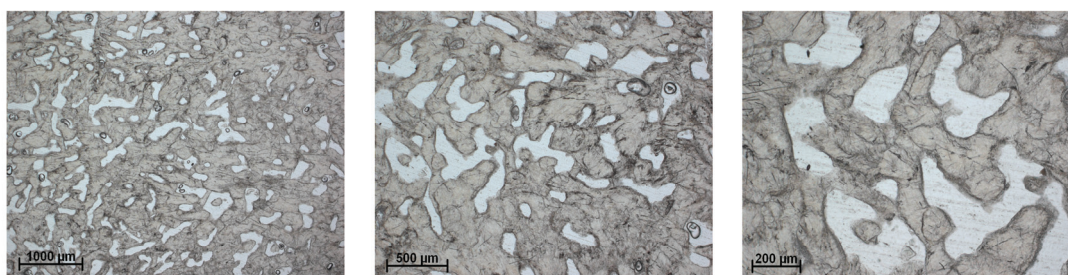
Supplementary Figure 2. Thin section photomicrographs of fossil Great Barrier Reef corals. Thin sections of *Isopora palifera*/*cuneata* corals are shown under transmitted light. No significant amounts of secondary aragonite or calcite cements are observed in the skeletal pore spaces, resulting in excellent preservation of primary porosity. **a,** Corals microsampled at subseasonal resolution. **b,** Corals microsampled for bulk composition.

325-53A-9R-CC (0-7)
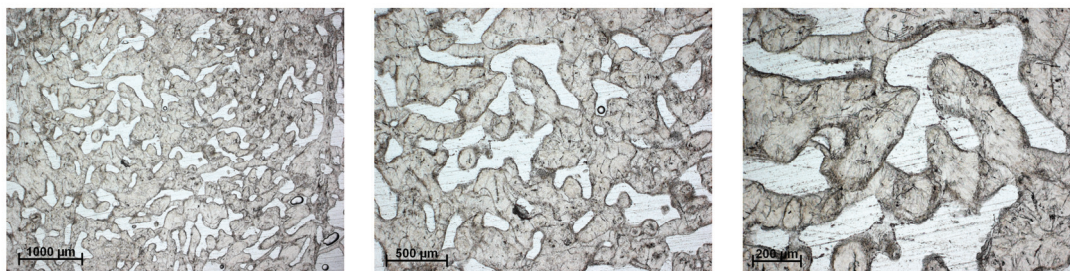
325-53A-15R-1 (33-37)
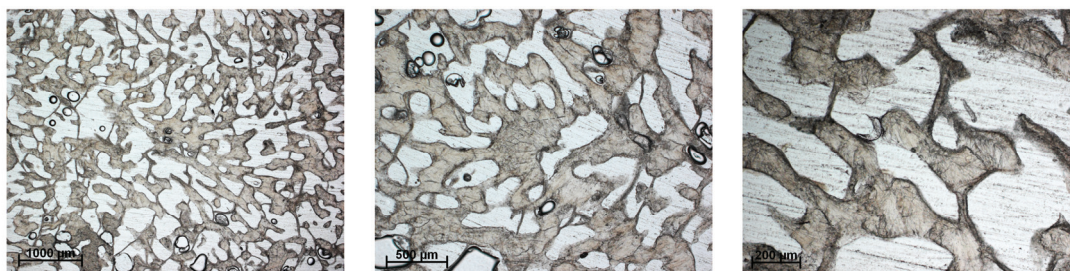
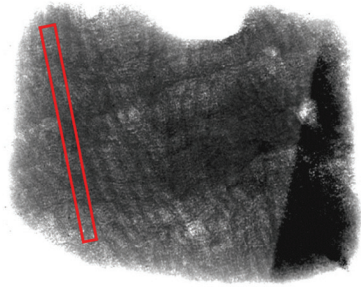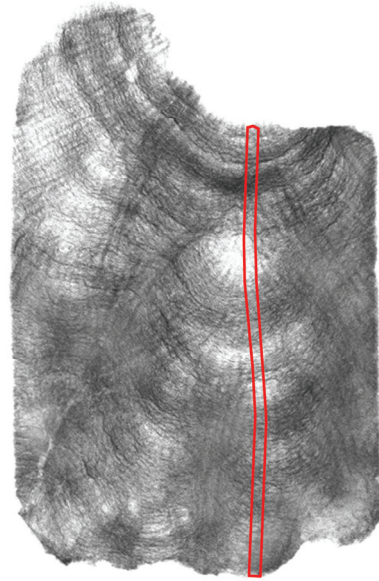## 325-57A-5R-1 (126-133)
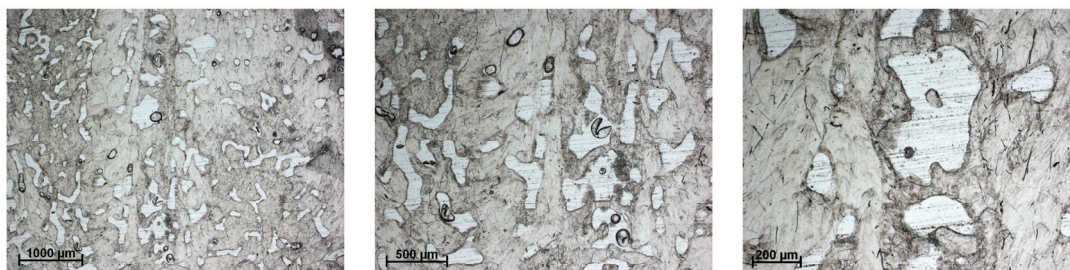
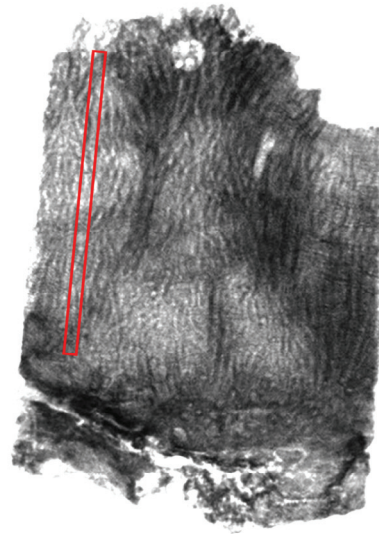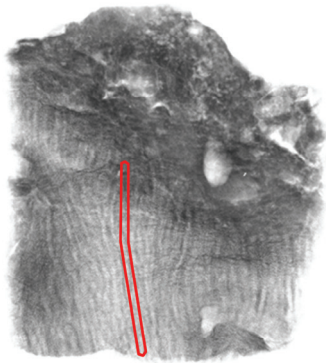**Supplementary Figure 2, a (continued).**

325-31A-2R-1 (27-32)
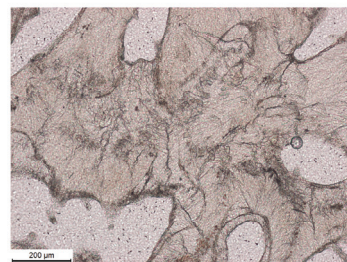
325-33A-5R-1 (68-74)
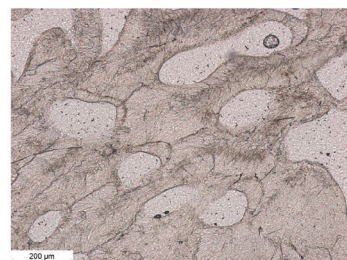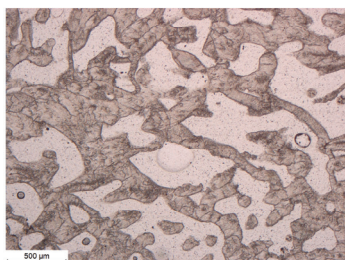
325-33A-9R-1 (7-16)
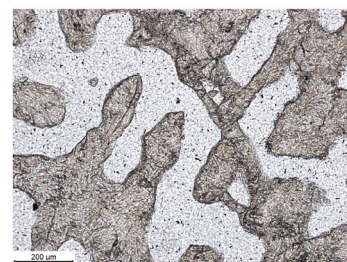
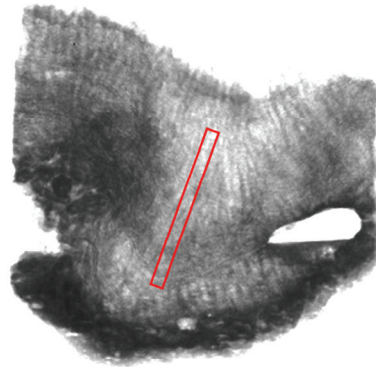

325-33A-10R-1 (42-48)
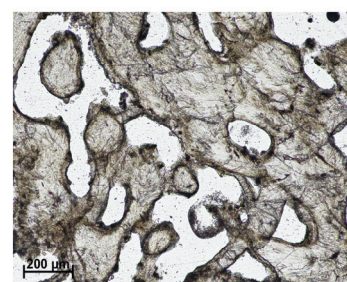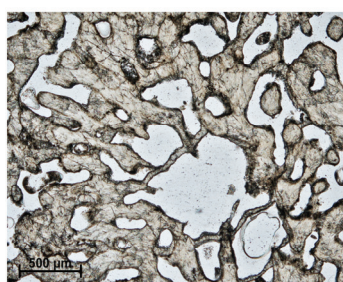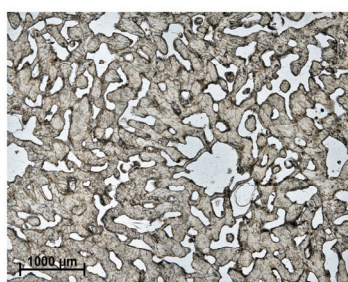
Supplementary Figure 2, b.

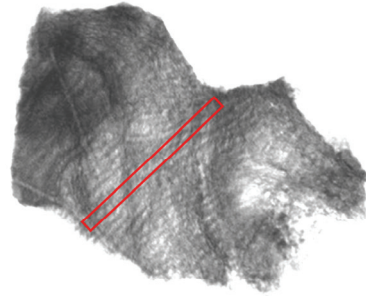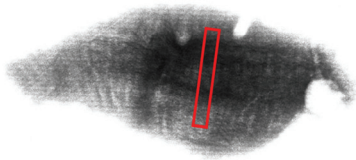325-33A-16R-1 (54-60)
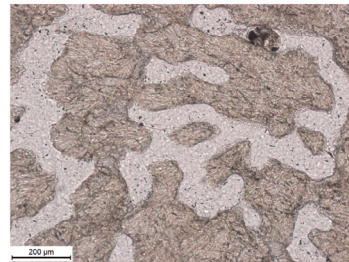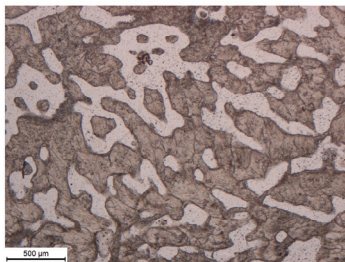
325-36A-16R-1 (6-10)
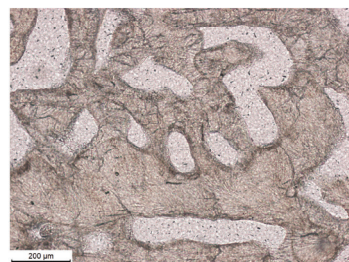
325-53A-6R-1 (7-9)
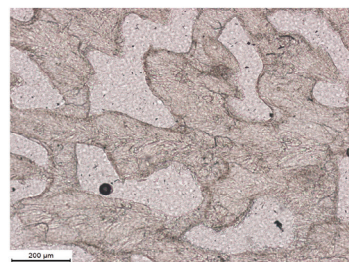
325-53A-15R-1 (30-33)
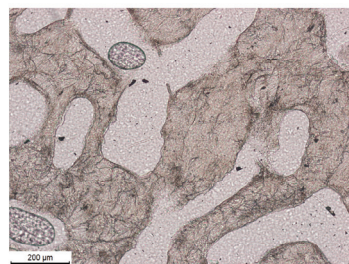
Supplementary Figure 2, b (continued).

325-57A-4R-1 (75-88)
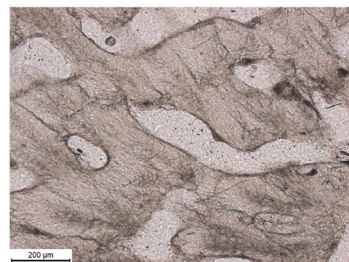
325-57A-5R-1 (1-3)
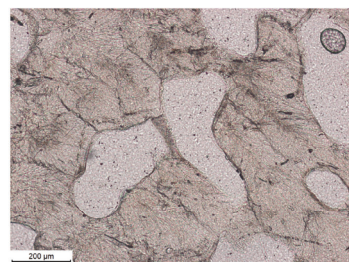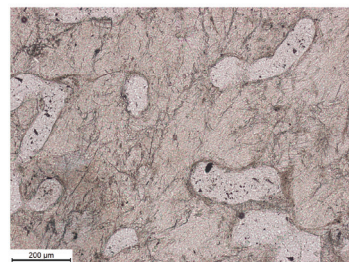
325-57A-5R-1 (41-50)

325-57A-5R-1 (115-122)
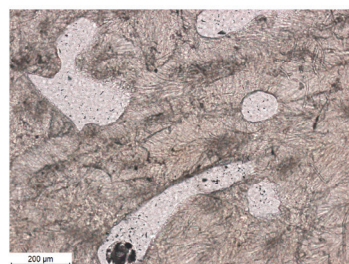
Supplementary Figure 2, b (continued).
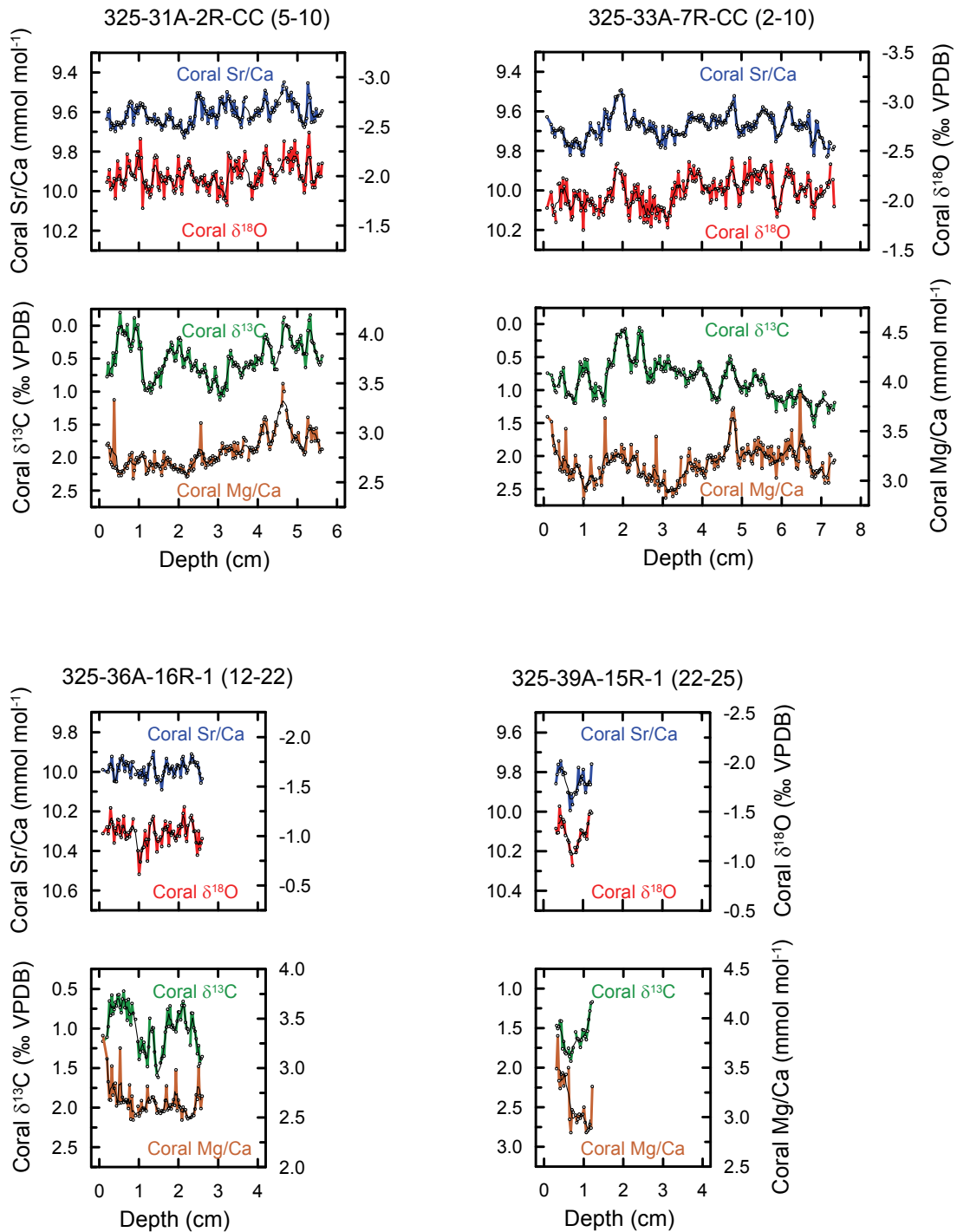
Supplementary Figure 3. Geochemical and isotopic records of fossil Great Barrier Reef corals. Records of Sr/Ca, $\delta^{18}O$, Mg/Ca, and $\delta^{13}C$ for *Isopora palifera/cuneata* corals analysed at subseasonal resolution. Records are shown relative to the distance from the start of the microsampling transect, which is located near the colony bottom. Thin black lines indicate 5-point running averages for corals 325-31A-2R-CC (5-10), 325-33A-7R-CC (2-10), and 325-39A-15R-1 (22-25), and 3-point running averages for all other corals. Note that the data shown were not corrected for the inter-laboratory offset, and represent the original data analysed at a single laboratory (MARUM, Bremen).

325-53A-9R-CC (0-7)

325-53A-15R-1 (33-37)

325-57A-5R-1 (126-133)
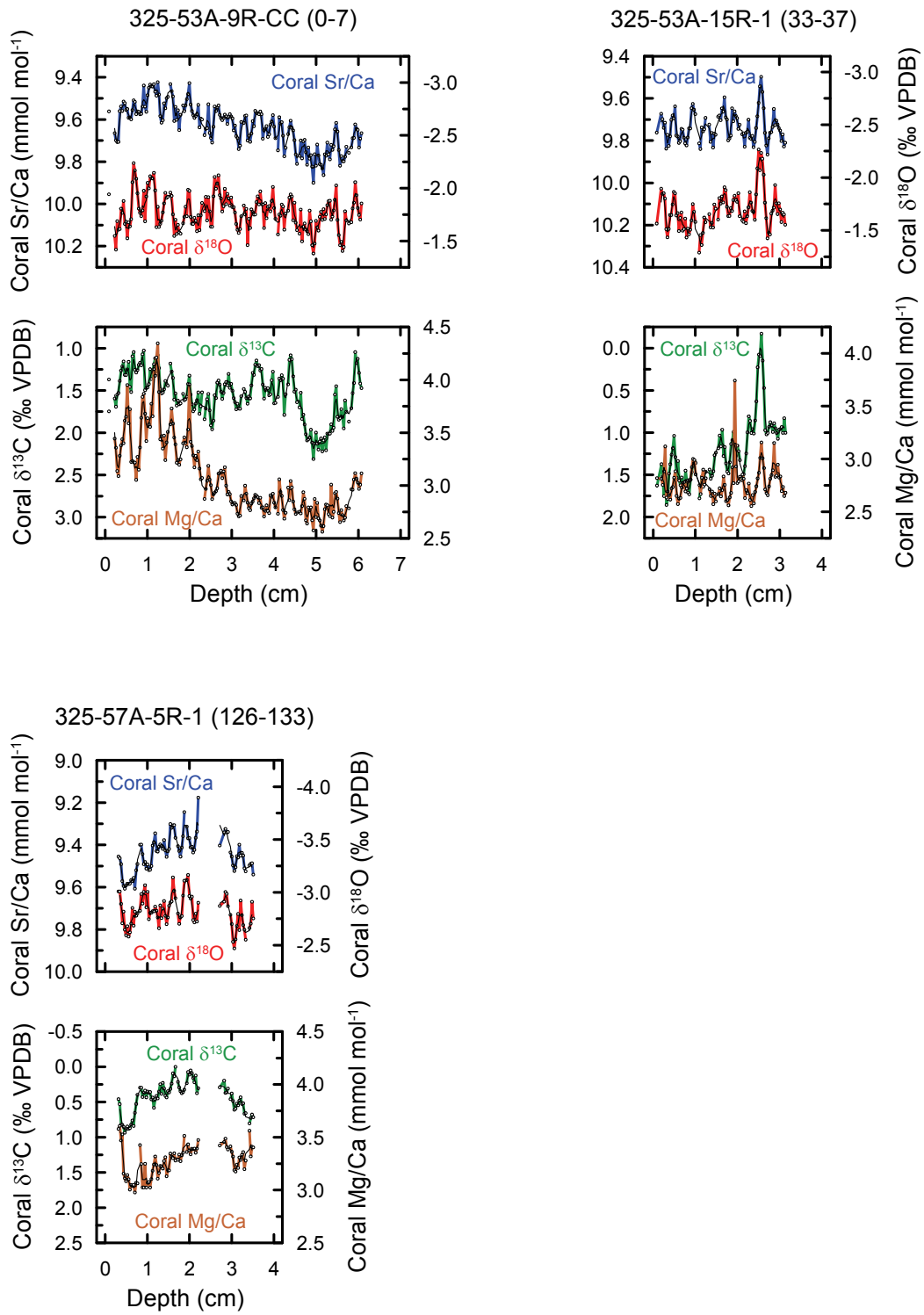
Supplementary Figure 3 (continued).
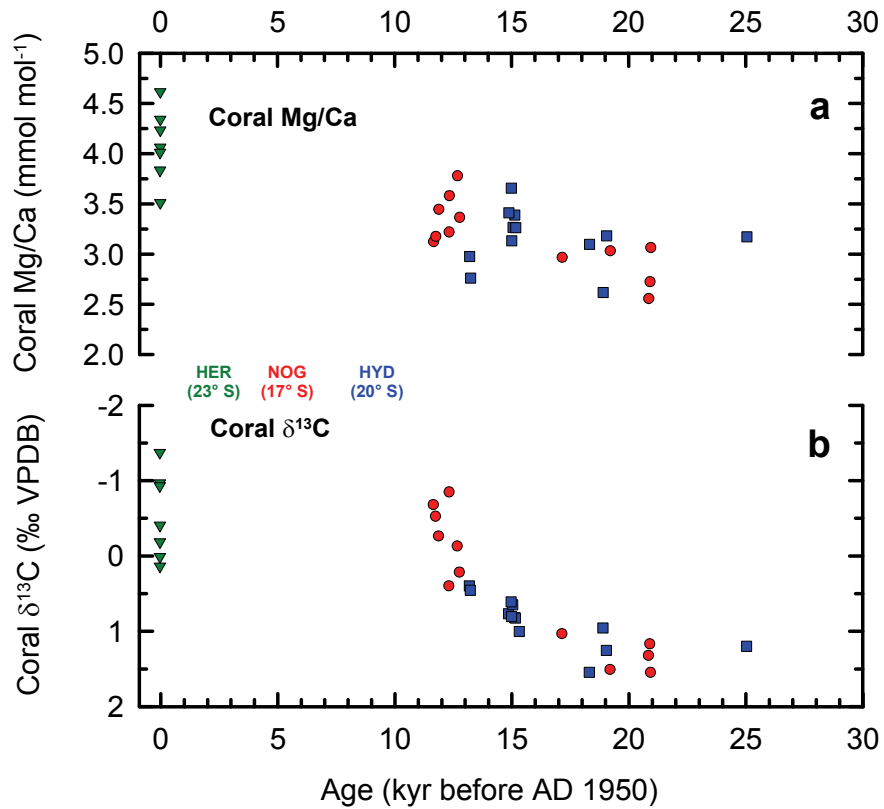
Supplementary Figure 4. Great Barrier Reef coral Mg/Ca and δ¹³C. a, Mean coral Mg/Ca of individual *Isopora palifera*/*cuneat*a colonies from Noggin Pass (NOG), Hydrographer's Passage (HYD), and Heron Island (HER). Approximate latitude is indicated. **b,** As in (**a**), but for mean coral δ¹³C.
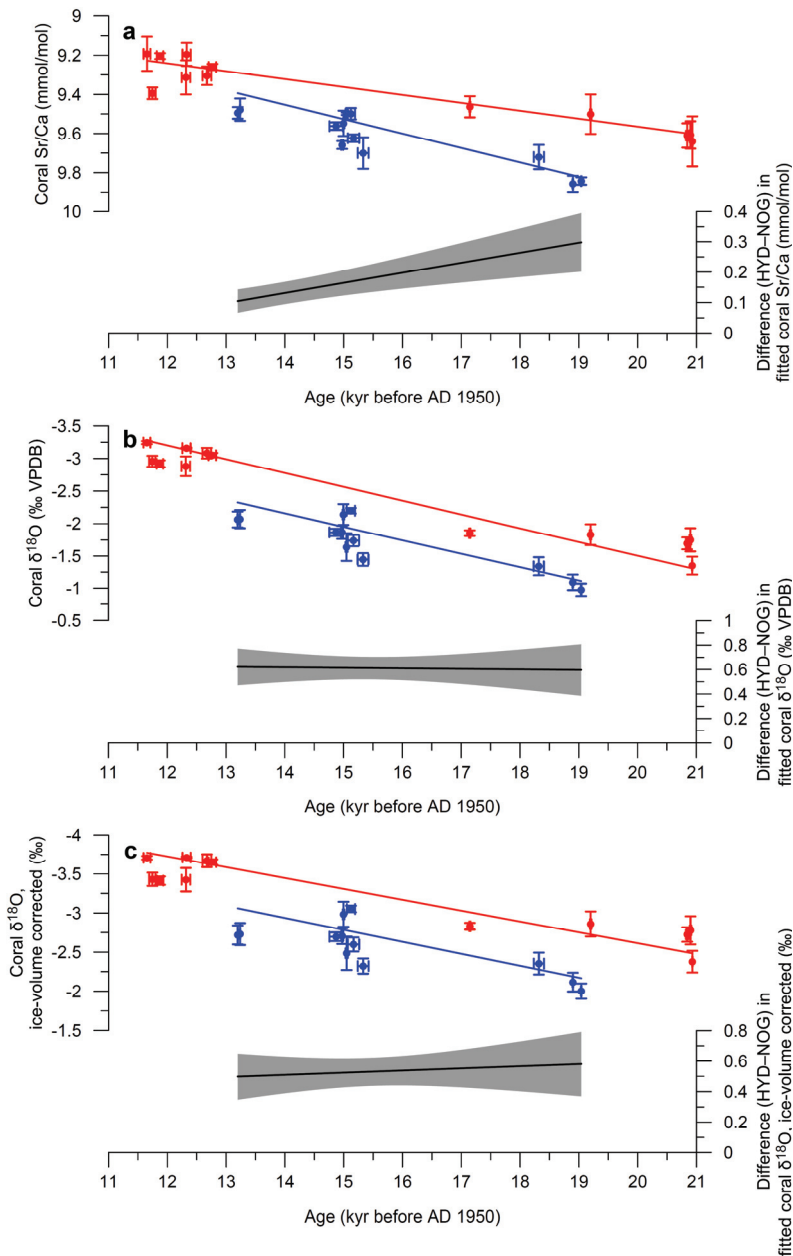
Supplementary Figure 5. Statistical regression analyses for coral Sr/Ca (a), $\delta^{18}O$ (b), and $\delta^{18}O$ corrected for ice volume influence (c). The coral data with 1-σ measurement errors were subjected to weighted least-squares regression (fits shown as solid lines). The difference in fit (shaded) is shown with the standard-error band resulting from a Monte Carlo simulation[1]. 400 simulations were performed with independent, normally distributed random deviations (standard deviation equal to dating error for age simulation and equal to measurement error × inflation factor for proxy simulation). In a conservative approach, to accommodate for unknown sources of uncertainty such as between-colony variability, the proxy measurement error was inflated by a factor of three. The coral data (NOG, red symbols; HYD, blue symbols) are shown with 1-σ measurement errors (proxy value, vertical bars) and 2-σ dating errors (age, horizontal bars).
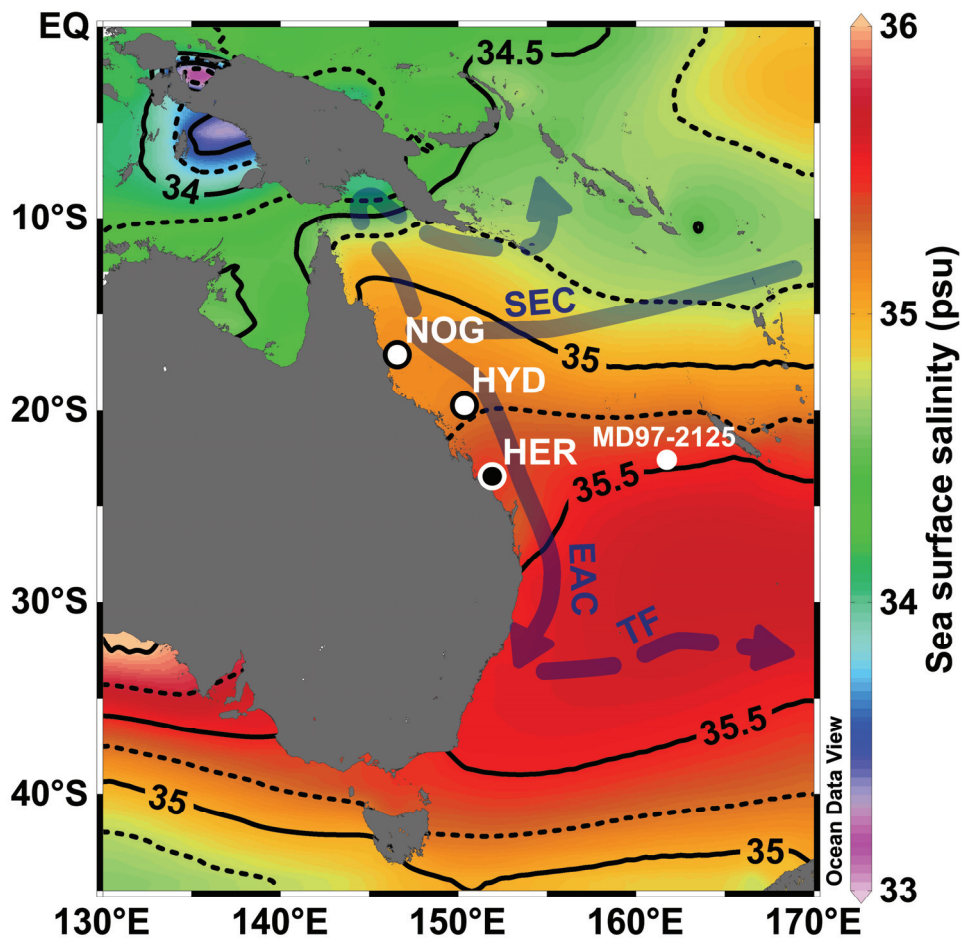
Supplementary Figure 6. Map of the south-western Pacific Ocean. Locations of
Integrated Ocean Drilling Program (IODP) Expedition 325 drilling sites at Noggin Pass
(NOG) and Hydrographer's Passage (HYD) in the central Great Barrier Reef[2] are
superimposed on annual mean sea surface salinity[3] and surface ocean circulation
patterns in the study area[4] (South Equatorial Current, SEC; East Australian Current,
EAC; Tasman Front, TF). For reference, the modern coral site at Heron Island (HER) in
the southern Great Barrier Reef is shown. The Coral Sea is the region off the northeast
coast of Australia that is bounded by New Guinea in the north and by several smaller
islands in the east.
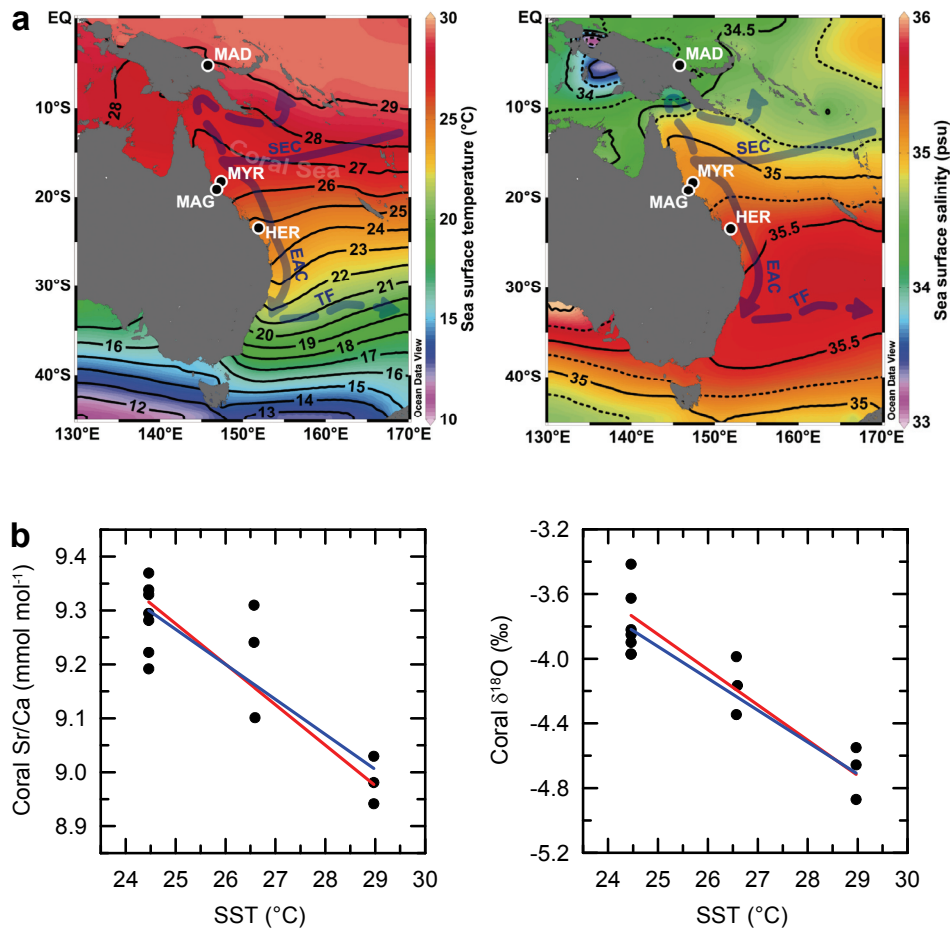
Supplementary Figure 7. Relationship between modern *Isopora* coral proxy data and sea surface temperature. a, Locations of modern coral sites at Heron Island (HER; 151.9° E, 23.4° S) in the southern Great Barrier Reef (GBR), Myrmidon Reef (MYR; 147.4° E, 18.3° S) and Magnetic Island (MAG; 146.8° E, 19.1° S) in the central GBR, and off Madang (MAD; 145.8° E, 5.2° S) on the north coast of Papua New Guinea are superimposed on annual mean sea surface temperature[5] (SST), annual mean sea surface salinity[3], and surface ocean circulation patterns in the study area[4] (South Equatorial Current, SEC; East Australian Current, EAC; Tasman Front, TF). **b,** Linear least-squares regression (blue lines) gives relationships of Sr/Ca × 10^3 = 10.89(±0.29) − 0.065(±0.011) × SST (r^2 = 0.75) and of δ^{18}O = 1.0(±0.7) − 0.197(±0.027) × SST (r^2 = 0.82). Reduced major axis regression (red lines) gives relationships of Sr/Ca × 10^3 = 11.15(±0.09) − 0.075(±0.011) × SST (r^2 = 0.75) and of δ^{18}O = 1.6(±0.5) − 0.218(±0.027) × SST (r^2 = 0.82). The regressions are based on robust branching/columnar *Isopora palifera/cuneata* colonies that were analysed for bulk composition, which were collected from 1974 to 1979 at depths between 0 and 14 m (HER), in 1982 at a depth of <15 m (MYR) and at a depth of <0.5 m (MAG), and in 1994 at depths between 4 and 15 m (MAD). Annual mean SST were derived from the World Ocean Atlas 2009 and represent the long-term climatological mean (1955-2006)[5]. Annual mean sea surface salinity[3] at MAD is ~1 psu lower relative to HER (Supplementary Fig. 6), which translates[6] into ~0.3‰ lower seawater δ^{18}O at MAD, resulting in a slight overestimation of the true δ^{18}O-SST sensitivity in our regression analysis.

17
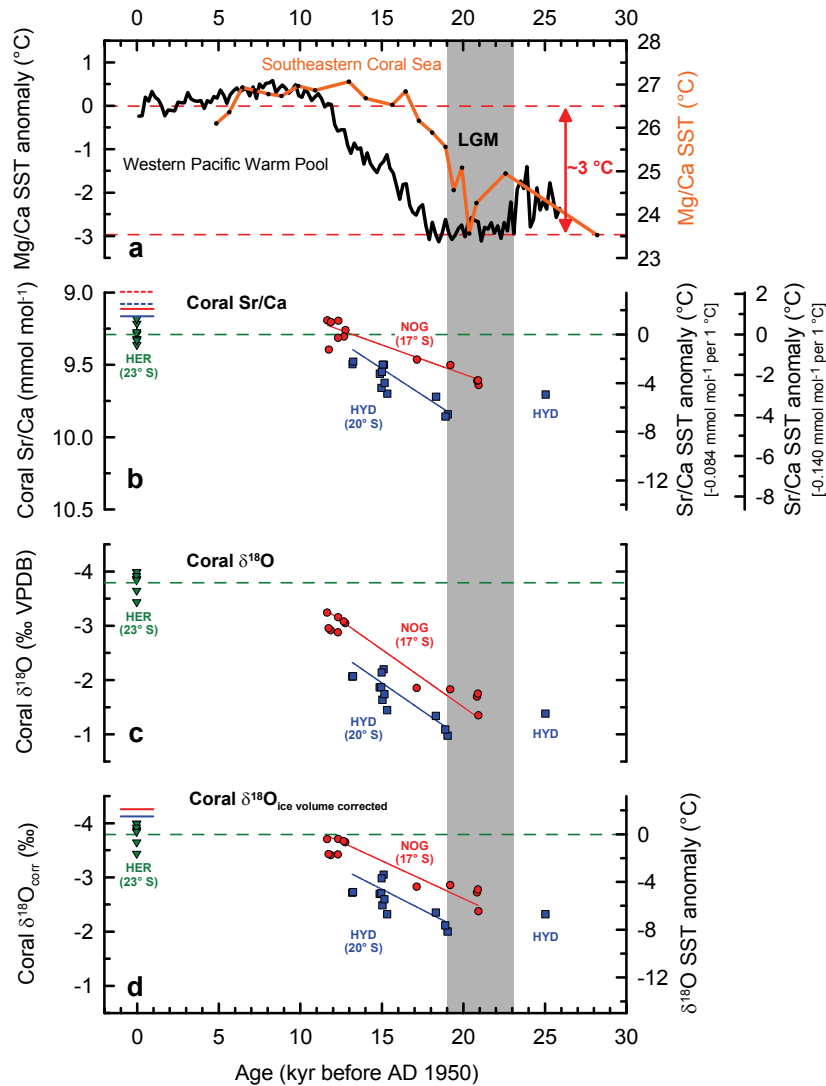
Supplementary Figure 8. Great Barrier Reef coral Sr/Ca and δ¹⁸O and western tropical Pacific temperatures. a, Western Pacific Warm Pool (WPWP) sea surface temperature (SST) anomaly[7] (left y-axis) and southeastern Coral Sea SST[8] (right y-axis) reconstructed from planktonic foraminiferal Mg/Ca. Modern annual mean WPWP SST is >4 °C warmer than SST in the southeastern Coral Sea[5]. **b,** Mean Sr/Ca of individual *Isopora palifera/cuneata* corals from Noggin Pass (NOG) and Hydrographer's Passage (HYD), central Great Barrier Reef (GBR), and Heron Island (HER), southern GBR (approximate latitude indicated). Weighted least-squares regression lines are shown for NOG and HYD, utilising data variances as weights. HYD coral Sr/Ca is significantly different from NOG coral Sr/Ca (Methods and Supplementary Fig. 5). The coral-based SST anomalies are not adjusted for changes in seawater Sr/Ca, and thus provide upper estimates of the magnitude of cooling. However, the effects of seawater Sr/Ca changes are similar at both sites, so the reconstructed SST differences between sites are not affected. For reference, the fossil coral-based Sr/Ca-SST anomalies are plotted relative to average Sr/Ca at HER (dashed green line). Modern mean SST[5] at NOG (26.6 °C) and HYD (26.0 °C) is shown relative to SST at HER (24.5 °C) and scaled using the mean coral Sr/Ca-SST relationships of –0.084 mmol mol⁻¹ per °C (ref. 9) (solid red and blue

lines) and –0.140 mmol mol^{-1} per °C (ref. 10) (dashed red and blue lines). **c,** As in (**b**), but for mean coral δ^{18}O. **d,** As in (**c**), but for mean coral δ^{18}O corrected for the influence of changes in ice volume using a global compilation of benthic foraminifer δ^{18}O records[11]. The resulting coral δ^{18}O-SST anomalies are shown relative to average δ^{18}O at HER (dashed green line) using the average of three mean coral δ^{18}O-SST relationships (–0.22‰ per °C, refs 9,10,12). The larger cooling inferred from coral δ^{18}O compared to Sr/Ca suggests a positive seawater δ^{18}O anomaly. Modern mean SST[5] at NOG and HYD is shown relative to HER (solid red and blue lines). The grey shading indicates the timing of the Last Glacial Maximum[13,14] (LGM).

Supplementary Table 1. Results of U-Th analysis.

Site	Sample ID Dating*	$(^{232}Th/^{238}U)$	± 2SD	$(^{234}U/^{238}U)$	± 2SD	$(^{230}Th/^{238}U)$	± 2SD	Laboratory**	Year Measured	U-Th Age$_{raw}$ [kyr BP]***	± 2SD	$(^{234}U/^{238}U)_{0\ raw}$	± 2SD	U-Th Age$_{detr.\ corr.}$ [kyr BP]***	± 2SD	$(^{234}U/^{238}U)_{0\ det.\ corr.}$	± 2SD
HYD	325-31A-2R-1 (27-32)	6.127E-06	3.635E-10	1.1412	0.0002	0.1308	0.00001	WHOI	2012	13.198	0.003	1.1466	0.0002	13.197	0.003	1.1466	0.0002
HYD	325-31A-2R-CC (5-10)	2.155E-06	1.938E-10	1.1408	0.0002	0.1311	0.00001	WHOI	2012	13.238	0.002	1.1462	0.0002	13.238	0.002	1.1462	0.0002
HYD	325-31A-7R-1 (16-24) A	3.7E-06	2.107E-10	1.1378	0.0002	0.1478	0.00001	WHOI	2012	15.089	0.003	1.1439	0.0002	15.088	0.003	1.1439	0.0002
HYD	325-31A-7R-1 (16-24) B	5.938E-06	3.586E-10	1.1384	0.0001	0.1485	0.00004	WHOI	2012	15.159	0.004	1.1445	0.0001	15.159	0.004	1.1445	0.0001
HYD	325-33A-5R-1 (68-74)	1.446E-05	8.029E-08	1.1366	0.0006	0.1466	0.00014	ANU	2012	14.975	0.017	1.1425	0.0006	14.974	0.017	1.1425	0.0006
HYD	325-33A-7R-CC (2-10)	3.345E-05	2.539E-07	1.1338	0.0005	0.1464	0.00010	ANU	2012	14.999	0.013	1.1396	0.0005	14.997	0.013	1.1396	0.0005
HYD	325-33A-8R-1 (13-17)	5.561E-06	8.351E-06	1.1397	0.0006	0.1461	0.00103	ANU	2012	14.875	0.113	1.1457	0.0006	14.871	0.113	1.1457	0.0006
HYD	325-33A-9R-1 (10-16)	2.197E-05	2.108E-07	1.1385	0.0010	0.1486	0.00087	OX	2011	15.169	0.085	1.1445	0.0011	15.167	0.097	1.1445	0.0011
HYD	325-33A-10R-1 (41-49)	2.128E-05	2.029E-07	1.1391	0.0010	0.1502	0.00083	OX	2011	15.333	0.080	1.1453	0.0011	15.331	0.092	1.1453	0.0011
HYD	325-33A-16R-1 (55-60)	7.702E-05	6.242E-07	1.1337	0.0010	0.2338	0.00127	OX	2011	25.044	0.133	1.1435	0.0012	25.038	0.156	1.1436	0.0011
HYD	325-35A-3R-1 (35-38)	2.703E-05	1.471E-07	1.1437	0.0010	0.1482	0.00010	ANU	2012	15.052	0.018	1.1500	0.0010	15.050	0.018	1.1500	0.0010
HYD	325-36A-16R-1 (6-10)	4.928E-05	2.727E-09	1.1348	0.0002	0.1827	0.00001	WHOI	2012	19.045	0.005	1.1423	0.0002	19.041	0.005	1.1423	0.0002
HYD	325-36A-16R-1 (13-22)	1.839E-05	2.835E-09	1.1344	0.0003	0.1814	0.00001	WHOI	2012	18.899	0.005	1.1418	0.0003	18.898	0.005	1.1418	0.0003
HYD	325-39A-15R-1 (22-25)	6.505E-05	6.282E-07	1.1364	0.0008	0.1767	0.00076	OX	2012	18.325	0.075	1.1437	0.0008	18.320	0.086	1.1437	0.0008
NOG	325-53A-6R-1 (7-9)	0.0002195	1.848E-08	1.1365	0.0001	0.1663	0.00002	WHOI	2012	17.163	0.003	1.1433	0.0001	17.146	0.011	1.1434	0.0001
NOG	325-53A-9R-CC (0-7) A	4.565E-05	3.014E-09	1.1348	0.0001	0.1841	0.00002	WHOI	2012	19.198	0.003	1.1423	0.0001	19.194	0.004	1.1423	0.0001
NOG	325-53A-9R-CC (0-7) B	2.099E-05	1.842E-09	1.1351	0.0002	0.1842	0.00001	WHOI	2012	19.208	0.004	1.1427	0.0002	19.207	0.004	1.1427	0.0002
NOG	325-53A-15R-1 (30-33)	0.0004321	2.594E-08	1.1337	0.0002	0.1985	0.00003	WHOI	2012	20.877	0.005	1.1419	0.0002	20.843	0.021	1.1419	0.0002
NOG	325-53A-15R-1 (33-37)	0.0002654	1.923E-08	1.1340	0.0002	0.1989	0.00004	WHOI	2012	20.920	0.006	1.1422	0.0002	20.899	0.014	1.1422	0.0002
NOG	325-53A-15R-1 (42-48)	1.405E-05	1.891E-09	1.1338	0.0002	0.1990	0.00002	WHOI	2012	20.931	0.004	1.1420	0.0002	20.930	0.004	1.1420	0.0002
NOG	325-57A-4R-1 (78-88)	3.48E-05	7.954E-07	1.1440	0.0013	0.1166	0.00054	OX	2011	11.657	0.048	1.1488	0.0013	11.655	0.059	1.1488	0.0013
NOG	325-57A-5R-1 (1-3)	4.458E-05	4.678E-07	1.1428	0.0007	0.1174	0.00050	OX	2012	11.749	0.048	1.1477	0.0008	11.746	0.054	1.1477	0.0008
NOG	325-57A-5R-1 (45-46)	0.000246	1.816E-06	1.1426	0.0007	0.1187	0.00051	OX	2012	11.895	0.048	1.1475	0.0008	11.875	0.055	1.1475	0.0008
NOG	325-57A-5R-1 (115-122)	0.0007088	1.55E-05	1.1415	0.0011	0.1232	0.00057	OX	2011	12.384	0.053	1.1465	0.0011	12.328	0.070	1.1466	0.0011
NOG	325-57A-5R-1 (126-133)	0.0002184	1.483E-06	1.1435	0.0010	0.1230	0.00067	OX	2011	12.334	0.063	1.1486	0.0011	12.317	0.073	1.1486	0.0011
NOG	325-57A-6R-1 (103-114)	0.0008169	1.788E-05	1.1414	0.0011	0.1265	0.00059	OX	2011	12.738	0.054	1.1466	0.0011	12.674	0.074	1.1466	0.0011
NOG	325-57A-6R-2 (66-80)	9.247E-05	2.048E-06	1.1434	0.0011	0.1271	0.00059	OX	2011	12.774	0.054	1.1487	0.0011	12.767	0.064	1.1487	0.0011

* Sample ID Dating can be slightly different to the corresponding Sample ID Palaeo (Supplementary Table 2), as the dating sample in some cases is a subsample of a larger coral section that was sampled for palaeoclimate.
** Woods Hole Oceanographic Institution (WHOI), Australian National University (ANU), University of Oxford (OX).
*** U-Th ages are reported as kyr before the present relative to AD 1950.

A, B: U-Th analyses were performed on different parts of the same coral specimen.
detr. corr.: Detritial corrected.
Results of powder X-ray diffraction (XRD) analysis are shown in Supplementary Table 2.
The corals are massive and robust/branching *Isopora palifera/cuneata* colonies.

Supplementary Table 2. Coral element/Ca and stable isotope data, U-Th ages, and XRD results.

Site	Sample ID Palaeo*	U-Th Age [kyr BP]**	± 2SD	Coral Sr/Ca [mmol/mol]	± 1SD	n	Coral δ^{18}O [‰ VPDB]	± 1SD	n	Coral δ^{18}O$_{corr}$ [‰] ice volume corr.	± 1SD	n	Coral Mg/Ca [mmol/mol]	± 1SD	n	Coral δ^{13}C [‰ VPDB]	± 1SD	n	Microsampling	Aragonite**** [%]
HYD	325-31A-2R-1 (27-32)	13.197	0.003	9.495	0.030	3	-2.06	0.12	3	-2.72	0.12	3	2.975	0.181	3	0.40	0.13	3	bulk	99.1
HYD	325-31A-2R-CC (5-10)	13.238	0.002	9.478	0.057	178	-2.07	0.14	178	-2.73	0.14	178	2.761	0.175	178	0.46	0.29	178	subseasonal	100
HYD	325-31A-7R-1 (16-24)	15.124	0.070 ***	9.499	0.029	3	-2.20	0.04	3	-3.05	0.04	3	3.389	0.293	3	0.82	0.09	3	bulk	98.7
HYD	325-33A-5R-1 (68-74)	14.974	0.017	9.659	0.020	3	-1.87	0.10	3	-2.71	0.10	3	3.657	0.191	3	0.61	0.20	3	bulk	99.3
HYD	325-33A-7R-CC (2-10)	14.997	0.013	9.548	0.065	232	-2.14	0.16	232	-2.98	0.16	232	3.132	0.173	232	0.81	0.29	232	subseasonal	100
HYD	325-33A-8R-1 (11-17)	14.871	0.113	9.562	0.019	3	-1.87	0.06	3	-2.70	0.06	3	3.412	0.080	3	0.77	0.10	3	bulk	98.5
HYD	325-33A-9R-1 (7-16)	15.167	0.097	9.624	0.019	3	-1.74	0.09	4	-2.60	0.09	4	3.263	0.216	3	0.82	0.13	4	bulk	99.5
HYD	325-33A-10R-1 (42-48)	15.331	0.092	9.700	0.080	3	-1.45	0.10	3	-2.32	0.10	3				1.00	0.03	3	bulk	100
HYD	325-33A-16R-1 (54-60)	25.038	0.156	9.706	0.007	3	-1.38	0.09	4	-2.32	0.09	4	3.172	0.153	3	1.20	0.06	4	bulk	99.7
HYD	325-35A-3R-1 (35-38)	15.050	0.018	9.499	0.006	2	-1.64	0.21	3	-2.49	0.21	3	3.267	0.011	2	0.65	0.07	3	bulk	99.1
HYD	325-36A-16R-1 (6-10)	19.041	0.005	9.843	0.019	3	-0.97	0.10	3	-2.00	0.10	3	3.181	0.092	3	1.25	0.08	3	bulk	99.0
HYD	325-36A-16R-1 (12-22)	18.898	0.005	9.857	0.041	77	-1.09	0.12	77	-2.12	0.12	77	2.617	0.160	77	0.96	0.28	77	subseasonal	100
HYD	325-39A-15R-1 (22-25)	18.320	0.086	9.720	0.062	29	-1.34	0.14	29	-2.35	0.14	29	3.097	0.257	29	1.55	0.19	29	subseasonal	>98.5
NOG	325-53A-6R-1 (7-9)	17.146	0.011	9.463	0.054	3	-1.85	0.04	3	-2.83	0.04	3	2.969	0.048	3	1.03	0.04	3	bulk	98.4
NOG	325-53A-9R-CC (0-7)	19.200	0.012 ***	9.501	0.101	188	-1.83	0.16	188	-2.86	0.16	188	3.034	0.361	188	1.51	0.28	188	subseasonal	100
NOG	325-53A-15R-1 (30-33)	20.843	0.021	9.610	0.062	3	-1.70	0.09	3	-2.72	0.09	3	2.558	0.049	3	1.32	0.05	3	bulk	98.5
NOG	325-53A-15R-1 (33-37)	20.899	0.014	9.607	0.070	94	-1.75	0.18	94	-2.78	0.18	94	2.726	0.163	94	1.17	0.39	94	subseasonal	100
NOG	325-53A-15R-1 (42-48)	20.930	0.004	9.640	0.128	3	-1.35	0.14	3	-2.38	0.14	3	3.066	0.200	3	1.54	0.07	3	bulk	98.5
NOG	325-57A-4R-1 (75-88)	11.655	0.059	9.193	0.088	3	-3.24	0.02	3	-3.71	0.02	3	3.125	0.174	3	-0.68	0.06	3	bulk	98.9
NOG	325-57A-5R-1 (1-3)	11.746	0.054	9.394	0.030	3	-2.96	0.08	3	-3.43	0.08	3	3.177	0.051	3	-0.53	0.15	3	bulk	99.2
NOG	325-57A-5R-1 (41-50)	11.875	0.055	9.204	0.015	3	-2.92	0.05	3	-3.41	0.05	3	3.447	0.013	3	-0.27	0.14	3	bulk	98.6
NOG	325-57A-5R-1 (115-122)	12.328	0.070	9.195	0.059	3	-3.16	0.01	2	-3.71	0.01	2	3.583	0.096	3	-0.85	0.07	2	bulk	98.6
NOG	325-57A-5R-1 (126-133)	12.317	0.073	9.313	0.087	83	-2.88	0.15	83	-3.42	0.15	83	3.221	0.151	83	0.40	0.23	83	subseasonal	99
NOG	325-57A-6R-1 (103-114)	12.674	0.074	9.305	0.047	7	-3.08	0.08	4	-3.67	0.08	4	3.780	0.193	7	-0.13	0.07	4	bulk	100
NOG	325-57A-6R-2 (66-80)	12.767	0.064	9.260	0.015	3	-3.05	0.03	3	-3.65	0.03	3	3.367	0.051	3	0.21	0.11	3	bulk	99.6
HER	GBR-206_bulk	-0.024		9.369		1	-3.63	0.10	3	-3.63	0.10	3	4.218		1	-0.38	0.01	3	bulk	
HER	GBR-219_bulk	-0.024		9.295		1	-3.97	0.04	2	-3.97	0.04	2	4.325		1	0.16	0.12	2	bulk	
HER	GBR-307_bulk	-0.024		9.329		1	-3.42	0.07	3	-3.42	0.07	3	3.494		1	0.03	0.06	3	bulk	
HER	GBR-318_bulk	-0.024		9.338		1	-3.85	0.04	2	-3.85	0.04	2	4.047		1	-0.16	0.01	2	bulk	
HER	GBR-537-bulk	-0.025		9.222		1	-3.97	0.04	2	-3.97	0.04	2	4.600		1	-0.94	0.05	2	bulk	
HER	GBR-947_bulk	-0.029		9.282		1	-3.82	0.01	2	-3.82	0.01	2	3.996		1	-0.91	0.05	2	bulk	
HER	GBR-954_bulk	-0.029		9.192		1	-3.90	0.01	2	-3.90	0.01	2	3.819		1	-1.35	0.17	2	bulk	
MAG	GBR-1023	-0.032		9.241	0.024	4	-4.35	0.04	3	-4.35	0.04	3				-1.42	0.07	3	bulk	
MAG	GBR-1024	-0.032		9.310	0.011	4	-3.99	0.06	3	-3.99	0.06	3				-1.56	0.01	3	bulk	
MYR	GBR-1108	-0.032		9.101	0.075	4	-4.17	0.11	3	-4.17	0.11	3				-0.72	0.09	3	bulk	
MAD	PNG-21A	-0.044		8.981	0.006	4	-4.55	0.07	3	-4.55	0.07	3				-2.30	0.04	3	bulk	
MAD	PNG-36	-0.044		9.030	0.015	4	-4.66	0.06	3	-4.66	0.06	3				-1.13	0.04	3	bulk	
MAD	PNG-89B	-0.044		8.942	0.012	4	-4.87	0.10	3	-4.87	0.10	3				-2.14	0.18	3	bulk	

* Sample ID Palaeo can be slightly different to the corresponding Sample ID Dating (Supplementary Table 1), as the dating sample in some cases is a subsample of a larger coral section that was sampled for palaeoclimate.

** U-Th ages are reported as kyr before the present relative to AD 1950.

*** U-Th age represents the mean of 2 datings, the error given here is the range of the two datings.

**** Results of powder X-ray diffraction (XRD) analysis.

The coral reference material JCp-1 was used to correct for inter-laboratory offsets. The JCp-1 reference compositions used in this study are 8.781 mmol mol^{-1} for Sr/Ca, –4.75‰ for δ^{18}O, 4.252 mmol mol^{-1} for Mg/Ca, and –1.58‰ for δ^{13}C.

The corals are massive and robust/branching *Isopora palifera/cuneata* colonies.

Supplementary Note 1

Between-colony offsets

The modern *Isopora palifera/cuneata* corals from HER (n = 7) reveal between-colony offsets in mean Sr/Ca and $\delta^{18}O$ that are on the same order as those for a group of fossil corals from HYD that grew ~15 kyr BP (n = 7) (Fig. 2). The maximum offset in mean Sr/Ca observed between modern corals at HER is 0.177 mmol mol^{-1}, which equates to an apparent sea surface temperature (SST) difference of 1-2 °C (refs 9,10,12; Fig. 2 and Supplementary Fig. 7). Consequently, we would not expect modern coral Sr/Ca-SST reconstructions to detect a difference of less than 0.6 °C in SST between the southern site (HYD) and northern site (NOG)[5] (Fig. 1). In contrast, the temperature difference between HYD and NOG inferred from the mean Sr/Ca of the fossil corals for the Last Glacial Maximum (LGM) and the last deglaciation are larger than the between-colony offsets (Fig. 2). The between-colony offsets in modern *Isopora* are well constrained at HER where a total of 7 different coral colonies were analysed, whereas the number of colonies analysed at the two other Great Barrier Reef (GBR) sites is ≤2 (Supplementary Fig. 7). Thus we use the average Sr/Ca and $\delta^{18}O$ of corals from HER as the benchmark to infer last deglacial SST changes in the central GBR, and take into account the modern SST difference between HER and the central GBR.

Supplementary Note 2

***Isopora* corals as sea surface temperature archive**

Coral skeletal Sr/Ca is a powerful proxy for reconstructing past changes in SST. Most previous work on this topic is based on analysis of *Porites* corals. As a consequence, the Sr/Ca-SST relationship for this genera is well known and constrained[9,10,12,15,16]. There are no existing analogous databases for the *Isopora palifera/cuneata* corals used in the present study. Therefore, we performed an initial calibration for these *Isopora* corals by comparing mean Sr/Ca and $\delta^{18}O$ from modern robust branching/columnar colonies from northern Papua New Guinea (Madang), the central GBR (Myrmidon Reef and Magnetic Island) and the southern GBR (Heron Island). These sites span a range of ~4.5 °C in annual mean SST. The modern corals were collected between 1974 and 1994, at water depths ranging between 0 and 15 m, and from each coral we sampled across several years of growth in an identical manner

to our sampling of the fossil corals in our study. Therefore, the modern coral sampling strategy captures a similar level of uncertainty to that associated with the fossil corals: sampling of different precise time intervals and corals representing a range of shallow water habitats on the reef. The resulting modern coral data (Supplementary Fig. 7) indicate that the Sr/Ca-SST and δ^{18}O-SST relationships in *Isopora* are similar to those of *Porites* corals, with the *Isopora* Sr/Ca bulk calibration slope closer to the seasonal *Porites* slope than to the bulk *Porites* slope. Furthermore, seasonal Sr/Ca calibration slopes similar to *Porites* were reported for a coral in the same family as *Isopora*, *Acropora palmata*[17], and early studies found similar Sr/Ca and δ^{18}O bulk calibration slopes for *Acropora* and *Porites*[18,19]. Therefore, we use the better-constrained mean *Porites* calibrations as the basis for estimating changes in SST through the last deglaciation. Crucially, our results on changes in meridional SST gradient through time are not dependent upon the details of the Sr/Ca-SST and δ^{18}O-SST relationships, and we would have reached identical conclusions using the modern *Isopora* data.

Supplementary Discussion

We find that shelf-edge SST logger data (loggers deployed by Australian Institute of Marine Science) on the modern GBR are in good agreement with the gridbox SST-based estimates[5] of current SST gradients (Fig. 1). The logger records show that modern-day inner shelf waters do exhibit a stronger meridional SST gradient than shelf-edge waters, but this is likely due to shallow-water effects on a wide shelf, which is not a valid analogue for the low sea level fringing reefs that existed along the steep front of the GBR, and absent wide shelf, during the LGM and last deglaciation.

Studies on modern corals in the GBR find no detectable impact of seasonal freshwater discharge from the continent on Sr/Ca ratios in inner- and mid-shelf corals[20-24]. These studies show that nearshore (Orpheus Island, Pandora Reef) corals analysed for Sr/Ca and δ^{18}O through dry and very wet years have a clear signal of river runoff in the coral δ^{18}O anomaly during the wet years, but no significant effect on coral Sr/Ca as a temperature proxy[20-22]. These findings are supported by evidence from Papua New Guinea where modern corals directly affected by high volumes of runoff from the Sepik River do not have a notable influence on the coral Sr/Ca temperature signal[25]. The results from the GBR and Papua New Guinea demonstrate the robustness of coral Sr/Ca

as temperature proxy even in environments heavily influenced by continental freshwater discharge. Furthermore, the Sr/Ca of our fossil GBR corals is not thought to be affected by mixing with a dissolved riverine flux of Sr, or Ca, because a freshwater component would be clearly evident in the $\delta^{18}O$ data. Furthermore, Sr/Ca in our fossil GBR corals is unlikely to have been influenced by changes in proximity to the shoreline consequent on sea level change, since during the glacial, although the corals would be closer to shore, they are also closer to open-ocean waters where freshwater plumes would be more rapidly mixed.

Supplementary References

1. Mudelsee, M. *Climate Time Series Analysis: Classical Statistical and Bootstrap Methods* 474 p. (Springer, Dordrecht, 2010).

2. Webster, J. M., Yokoyama, Y., Cotteril, C. & the Expedition 325 Scientists. *Proc. IODP, Vol.* **325.** (Integrated Ocean Drilling Program Management International, Inc., Tokyo) doi:10.2204/iodp.proc.325.2011 (2011).

3. Antonov, J. I. *et al.* World Ocean Atlas 2009, Vol. 2: Salinity. *NOAA Atlas NESDIS 69* (ed. S. Levitus) 184 p. (U.S. Gov. Printing Office, Washington, D.C., 2010).

4. Hill, K. L., Rintoul, S. R., Ridgway, K. R. & Oke, P. R. Decadal changes in the South Pacific western boundary current system revealed in observations and ocean state estimates. *J. Geophys. Res. Oceans* **116,** C01009 (2011).

5. Locarnini, R. A. *et al.* World Ocean Atlas 2009, Vol. 1: Temperature. *NOAA Atlas NESDIS 68* (ed. S. Levitus) 184 p. (U.S. Gov. Printing Office, Washington, D.C., 2010).

6. Fairbanks, R. G. *et al.* Evaluating climate indices and their geochemical proxies measured in corals. *Coral Reefs* **16,** S93-S100 (1997).

7. Linsley, B. K., Rosenthal, Y. & Oppo, D. W. Holocene evolution of the Indonesian throughflow and the western Pacific warm pool. *Nature Geosci.* **3,** 578-583 (2010).

8. Tachikawa, K., Vidal, L., Sonzogni, C. & Bard, E. Glacial/interglacial sea surface temperature changes in the Southwest Pacific ocean over the past 360 ka. *Quat. Sci. Rev.* **28,** 1160-1170 (2009).

9.   Gagan, M. K., Dunbar, G. B. & Suzuki, A. The effect of skeletal mass accumulation in *Porites* on coral Sr/Ca and $\delta^{18}O$ paleothermometry. *Paleoceanography* **27,** PA1203 (2012).

10.   Felis, T. *et al.* Subtropical coral reveals abrupt early-twentieth-century freshening in the western North Pacific Ocean. *Geology* **37,** 527-530 (2009).

11.   Waelbroeck, C. *et al.* Sea-level and deep water temperature changes derived from benthic foraminifera isotopic records. *Quat. Sci. Rev.* **21,** 295-305 (2002).

12.   DeLong, K. L., Quinn, T. M., Shen, C.-C. & Lin, K. A snapshot of climate variability at Tahiti at 9.5 ka using a fossil coral from IODP Expedition 310. *Geochem. Geophys. Geosyst.* **11,** Q06005, doi:10.1029/2009GC002758 (2010).

13.   Mix, A. C., Bard, E. & Schneider, R. Environmental processes of the ice age: land, oceans, glaciers (EPILOG). *Quat. Sci. Rev.* **20,** 627-657 (2001).

14.   MARGO Project Members. Constraints on the magnitude and patterns of ocean cooling at the Last Glacial Maximum. *Nature Geosci.* **2,** 127-132 (2009).

15.   Beck, J. W. *et al.* Sea-surface temperature from coral skeletal strontium/calcium ratios. *Science* **257,** 644-647 (1992).

16.   Corrège, T. Sea surface temperature and salinity reconstruction from coral geochemical tracers. *Palaeogeogr., Palaeoclimatol., Palaeoecol.* **232,** 408-428 (2006).

17.   Gallup, C. D. *et al.* Sr/Ca-Sea surface temperature calibration in the branching Caribbean coral *Acropora palmata*. *Geophys. Res. Lett.* **33,** L03606 (2006).

18.   Weber, J. N. & Woodhead, P. M. J. Temperature dependence of oxygen-18 concentration in reef coral carbonates. *J. Geophys. Res.* **77,** 463-473 (1972).

19.   Weber, J. N. Incorporation of strontium into reef coral skeletal carbonate. *Geochim. Cosmochim. Acta* **37,** 2173-2190 (1973).

20.   McCulloch, M. T., Gagan, M. K., Mortimer, G. E., Chivas, A. R. & Isdale, P. J. A high-resolution Sr/Ca and $\delta^{18}O$ coral record from the Great Barrier Reef, Australia, and the 1982-1983 El Niño. *Geochim. Cosmochim. Acta* **58,** 2747-2754 (1994).

21.   Gagan, M. K. *et al.* Temperature and surface-ocean water balance of the mid-Holocene tropical western Pacific. *Science* **279,** 1014-1018 (1998).

22. Gagan, M. K. *et al.* Coral oxygen isotope evidence for recent groundwater fluxes to the Australian Great Barrier Reef. *Geophys. Res. Lett.* **29,** 1982 (2002).

23. Alibert, C. *et al.* Source of trace element variability in Great Barrier Reef corals affected by the Burdekin flood plumes. *Geochim. Cosmochim. Acta* **67,** 231-246 (2003).

24. Fallon, S. J., McCulloch, M. T. & Alibert, C. Examining water temperature proxies in *Porites* corals from the Great Barrier Reef: a cross-shelf comparison. *Coral Reefs* **22,** 389-404 (2003).

25. Ayliffe, L. K. *et al.* Geochemistry of coral from Papua New Guinea as a proxy for ENSO ocean–atmosphere interactions in the Pacific Warm Pool. *Cont. Shelf Res.* **24,** 2343-2356 (2004).